Structure and Optical Properties of TiO_2 Containing Oxide Glasses

K. Inoue[1], S. Sakida[2], T. Nanba[1], Y. Miura[1]

[1]Department of Environmental Chemistry and Materials, Okayama University
3-1-1, Tsushima-Naka, Okayama 700-8530, Japan
[2]Health and Environment Center, Okayama University
3-1-1, Tsushima-Naka, Okayama 700-8530, Japan

keywords: titanosilicate glass, refractive index, refractive index dispersion, coordination structure

Abstract

Refractive index and dispersion in R_2O–TiO_2–SiO_2 glass systems were investigated. The compositional dependence in the refractive index and dispersion was successfully expressed by the single-oscillator Drude-Voigt equation, where it was found that the average resonance wavelength λ_0 was the predominant parameter for both the refractive index and dispersion. It was suggested from Raman spectra that low TiO_2 content glasses were abundant in TiO_4 units, and with increasing TiO_2 content, the relative amount of TiO_5 and TiO_6 units increased. Structural model was proposed to reproduce the experimental findings in Raman and X-ray photoelectron spectra.

1. Introduction

By the addition of TiO_2 to a glass, various properties of the glass are modified; for example, increase in refractive index, decrease in thermal expansion coefficient, and expansion of glass forming region. It also enables to provide an athermal property (no temperature dependence of the optical path length) and a high third-order nonlinear optical susceptibility. In addition, second-order nonlinearity can be given by thermal poling. TiO_2-containiing glasses are expected as alternatives of Pb-containing glasses and optical materials, and they have been extensively studied in recent years.

In oxide glasses, Ti^{4+} ions take various coordinate structures as TiO_4, TiO_5 and TiO_6, resulting in the specific characteristics. Ti ions in tetrahedral TiO_4 units are regarded as network former (NWF), and those in octahedral TiO_6 units are as network modifier (NWM). Ti ions in TiO_5 units play an intermediate role between NWF and NWM. TiO_5 units are in a tetragonal pyramid structure with an extremely short Ti–O bond in the axial direction. The oxygen atom in the axial Ti–O bond is regarded as non-bridging oxygen (NBO), and the rest are attributed to bridging oxygen (BO).

A number of reports have been published concerning the coordination structures of Ti ions in glass. Sakka et al. [1,2] reported that most Ti ions existed in TiO_4 units in K_2O–TiO_2 and Cs_2O–TiO_2 glass systems. Kusabiraki et al. [3] reported that coordination number of Ti ions in Na_2O–TiO_2–SiO_2 glasses changed from 4 to 6 with increasing Na_2O content. There remain unresolved questions such as the relation between coordination structure of Ti and optical properties. Then, in the present study, the correlation between the glass structure and the optical properties has been investigated in R_2O–TiO_2–SiO_2 glass systems. Refractive index and dispersion were examined by using the single-oscillator Drude-Voigt equation. Glass structure and electronic state were evaluated on the basis of X-ray photoelectron spectroscopy (XPS), Raman scattering and nuclear magnetic resonance (NMR). The influence of the structures on the optical properties was finally discussed.

2. Theory

Refractive index dispersion was analyzed by the Drude-Voigt equation. According to the single-oscillator Drude-Voigt dispersion equation [4,5], refractive index n is related to the frequency of light ω,

$$n^2 - 1 = \frac{4\pi N e^2}{m} \cdot \frac{f}{\omega_0^2 - \omega^2} \qquad (1)$$

where e and m are the electronic charge and mass, respectively, N is the number of molecules in a unit volume, f is the average oscillator strength, and ω_0 is the average resonance frequency. Eq. 1 is rewritten into more convenient form.

$$\frac{1}{n_\lambda^2 - 1} = -\left(\frac{\pi m c^2}{e^2}\right) \cdot \left(\frac{1}{Nf}\right) \cdot \frac{1}{\lambda^2} + \left(\frac{\pi m c^2}{e^2}\right) \cdot \left(\frac{1}{Nf\lambda_0^2}\right) \qquad (2)$$

where c is the velocity of light, λ_0 is the average resonance wavelength, λ is the wavelength of light. It is expected from Eq. 2 that if $1/(n^2-1)$ is plotted against $1/\lambda^2$, a linear correlation is obtained, and the parameters λ_0 and Nf are determined from the intercept and slope. The number of molecules in a unit volume, N, is calculated from density. As a result, three parameters, N, f and λ_0 can be calculated.
In the region far away from λ_0, ($\lambda \gg \lambda_0$), Eq. 2 is simplified as

$$n^2 - 1 = \frac{e^2}{\pi m c^2} Nf\lambda_0^2 \qquad (3)$$

Consequently, a linear relationship is also expected between n^2 and $Nf\lambda_0{}^2$.
Abbe number is the wavelength dispersion of refractive index, which is given by

$$\nu_d = \frac{(n_d - 1)}{(n_F - n_c)} \qquad (4)$$

where ν_d is the Abbe number, and n_d, n_F and n_c indicate the refractive indexes at λ = 587.6, 486.1 and 656.3 nm, respectively. Larger ν_d value represents smaller dispersion. By using Eq. 2, Eq. 4 is rewritten as

$$\nu_d = \frac{\left(1/\lambda_0{}^2 - 1/\lambda_F{}^2\right)\left(1/\lambda_0{}^2 - 1/\lambda_c{}^2\right)}{\left(1/\lambda_F{}^2 - 1/\lambda_C{}^2\right)\left(1/\lambda_0{}^2 - 1/\lambda_d{}^2\right)} \qquad (5)$$

where λ_d, λ_F and λ_c are the wavelengths of d (587.6), F (486.1) and c (656.3 nm) lines, respectively. Eq. 5 suggests that the dispersion is also dependent on the average resonance wavelength, λ_0.

3. Experimental Procedures

Table I shows the glass compositions prepared in this study. In series 1, 3 and 5, the alkali content was constant, and Ti were substituted for Si. And in series 2, 4 and 6, TiO_2 was added to alkali di-silicate

glasses. For comparison, some borate glasses were prepared. All the glasses were melted in a Pt crucible with a lid at 1300 ~ 1500 °C for silicate glasses and 1100 ~ 1200 °C for borate glasses. The melts were poured into a graphite mold heated at the glass transition temperatures, and subsequently the glasses were annealed at near the glass temperatures. The glass surfaces on both sides were optically polished before measuring refractive index, density, Raman spectra and absorption spectra.

Table I. Compositions of Glasses Examined in This Study (molar ratio)		
[series 1]	$Li_2O{\cdot}2\{x_1TiO_2{\cdot}(1-x_1)SiO_2\}$	x_1=0, 0.1, 0.2, 0.3
[series 2]	$x_2TiO_2{\cdot}(1-x_2)\{Li_2O{\cdot}2SiO_2\}$	x_2=0, 0.1, 0.2, 0.3, 0.4, 0.5
[series 3]	$Na_2O{\cdot}2\{x_3TiO_2{\cdot}(1-x_3)SiO_2\}$	x_3=0, 0.1, 0.2, 0.3, 0.4, 0.5, 0.6
[series 4]	$x_4TiO_2{\cdot}(1-x_4)\{Na_2O{\cdot}2SiO_2\}$	x_4=0, 0.1, 0.2, 0.3, 0.4, 0.5, 0.6
[series 5]	$K_2O{\cdot}2\{x_5TiO_2{\cdot}(1-x_5)SiO_2\}$	x_5=0, 0.1, 0.2, 0.3, 0.4, 0.5, 0.6, 0.7, 0.8
[series 6]	$x_6TiO_2{\cdot}(1-x_6)\{K_2O{\cdot}2SiO_2\}$	x_6=0, 0.1, 0.2, 0.3, 0.4, 0.5, 0.6,0.7

Refractive index was measured with a prism coupler method (Metricon, Model 2010) at the wavelengths of 473.1, 632.8, 983.1 and 1548 nm. Density was determined by the Archimedes method using kerosene as an immersion liquid. Raman spectra were recorded using a RAMANORT64000 (Jovan Ibon). Absorption spectra were measured with V-570 UV-VIS spectrophotometer (Nihon-Bunko). XPS measurements were performed by using a S-Probe ESCA SSX-100S (Fisons Instruments) in a high vacuum of 10^{-8} Pa or less. ^{29}Si MAS NMR spectra were measured with ^{UNITY}INOVA300 (Varian), where 0.1 mol% of Fe_2O_3 was added to the glass batches for the NMR measurement.

4. Results and Discussion

4.1 Refractive Index and Density

The compositional dependence of the refractive index at 632.8 nm and density are shown in Figure 1, in which the data of a borate series are also shown. It is commonly observed that refractive index and density increase with increasing TiO_2 content. In series 4, a sharp rise in refractive index is seen at high TiO_2 region.

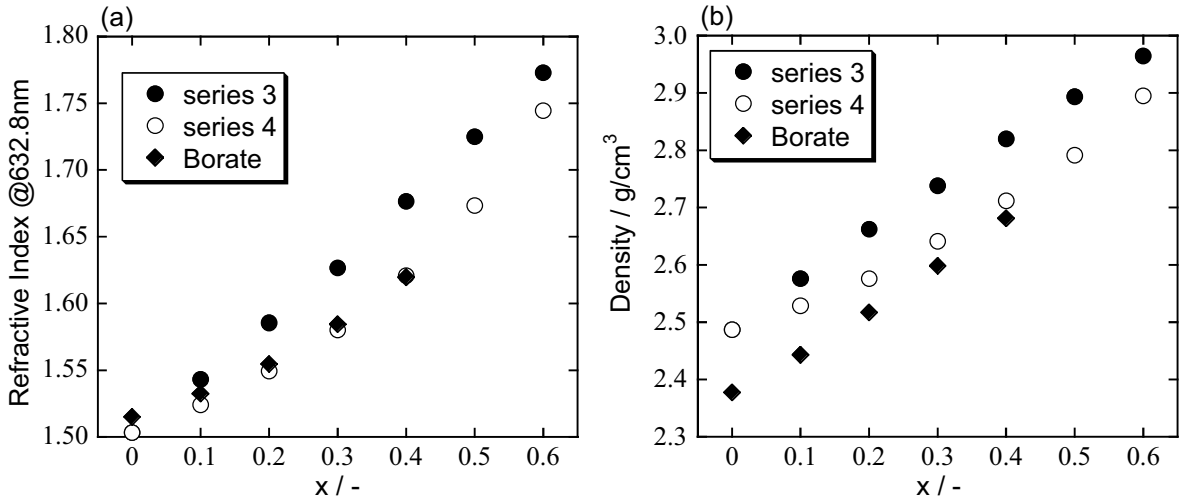

Figure 1: Compositional dependence of (a) refractive index and (b) density in the glasses of series 3: $Na_2O{\cdot}2\{x_3TiO_2{\cdot}(1-x_3)SiO_2\}$, series 4: $x_4TiO_2{\cdot}(1-x_4)\{Na_2O{\cdot}2SiO_2\}$ and borate: $Na_2O{\cdot}2\{xTiO_2{\cdot}(1-x)B_2O_3\}$.

4.2 Drude-Voigt Analyses of Refractive Index and Dispersion

As mentioned, according to the single-oscillator Drude-Voigt dispersion model [4,5], $1/(n^2-1)$ must be proportional to $1/\lambda^2$ as expressed in Eq. 2. Figure 2 shows the correlation between $1/(n^2-1)$ and $1/\lambda^2$ for the glasses in series 3. Linear relationship with high correlation coefficient $R > 0.999$ is confirmed in every glass, indicating that the Drude-Voigt model is applicable to the present glasses.

According to the simplified Drude-Voigt equation (Eq. 3), n^2 must be proportional to $Nf\lambda_0^2$ at the region $\lambda \gg \lambda_0$. Then, n^2 at λ = 1548 nm is plotted against $Nf\lambda_0^2$ in Figure 4(a), where a linear correlation is clearly recognized between n^2 and $Nf\lambda_0^2$. From the correlations shown in Figs. 4(b) ~ 4(d), it is also found that the average resonance wavelength, λ_0 is the predominant factor for determining the refractive index.

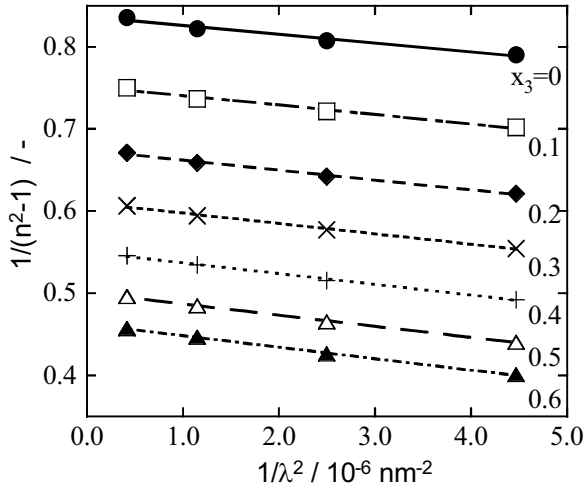

Figure 2: Correlation between $1/(n^2-1)$ and $1/\lambda^2$ for the glasses in series 3: $Na_2O{\cdot}2\{x_3TiO_2{\cdot}(1-x_3)SiO_2\}$. Lines are drawn by assuming the single-oscillator Drude-Voigt dispersion model expressed by Eq. 2.

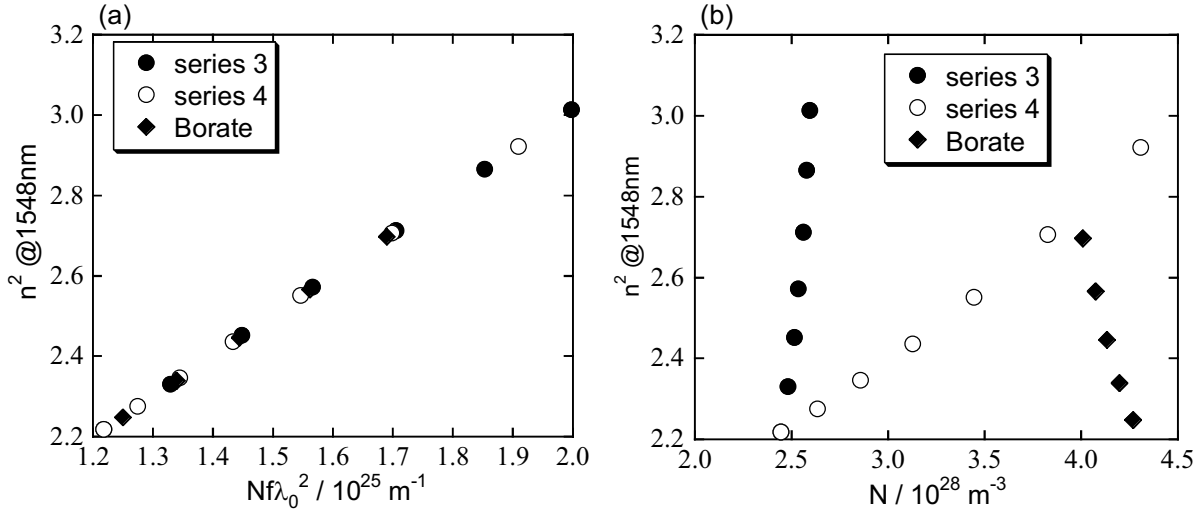

Figure 3: Correlation between n^2 at λ = 1548 nm and (a) $Nf\lambda_0^2$, (b) N, (c) f and (d) λ_0^2.
(continued to the next page)

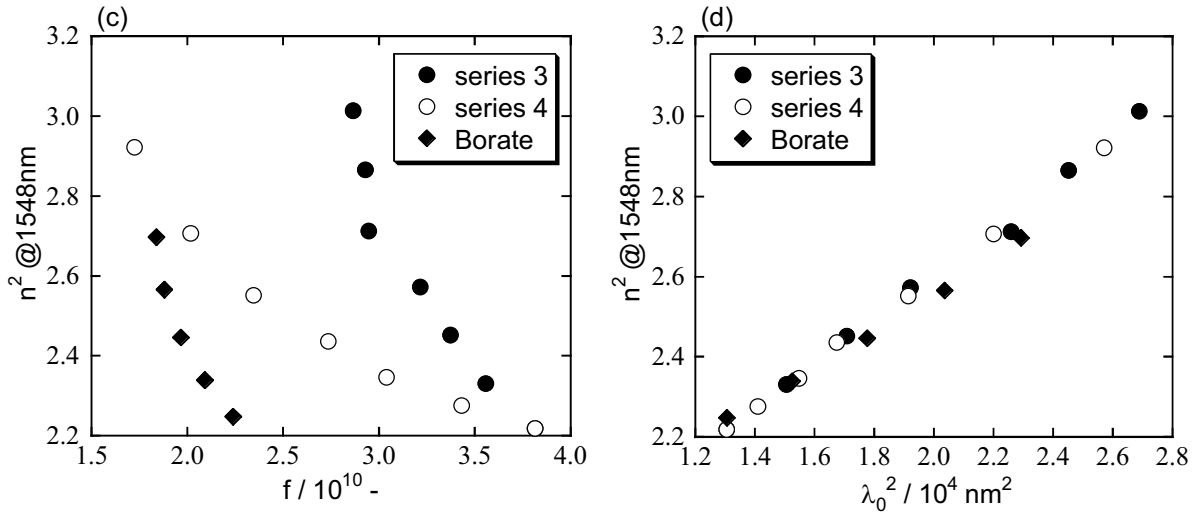

Figure 3: (continuation)

In the glasses shown in Fig. 3, the resonance wavelength λ_0 ranges between 110 and 170 nm, which is in vacuum UV region, and hence the direct experimental determination is quite difficult. According to Hirota et al. [6], the resonance wavelength of bridging oxygen is observed at 106 ~ 120 nm, and that of non-bridging oxygen is seen at 160 ~ 190 nm. Then, two interpretations are possible for the increase of λ_0 along with TiO_2 addition. One of them is the increase in NBO content in the glasses. If the resonance wavelength of Ti^{4+} ions is in the similar region to that of NBO, the increase in TiO_2 content should result in the increase in the average resonance wavelength λ_0.

In the TiO_2-containing glasses, the contributions of NBO 2p and Ti 4s+3d orbitals are probably large in HOMO and LUMO levels, respectively. Some correlation is, therefore, expected between λ_0 and wavelength at the optical absorption edge, λ_E.

Figure 4 shows the correlation between λ_0 and λ_E determined from absorption spectra. As TiO_2 content increases, λ_E increases and λ_0 also increases. At $\lambda_E < 340$ nm, a common correlation is observed even in the different sample series, and at $\lambda_E > 340$ nm, however, different correlations are confirmed between the different series, indicating that the average resonance wavelength is not always dominated by the optical absorption edge or optical bandgap.

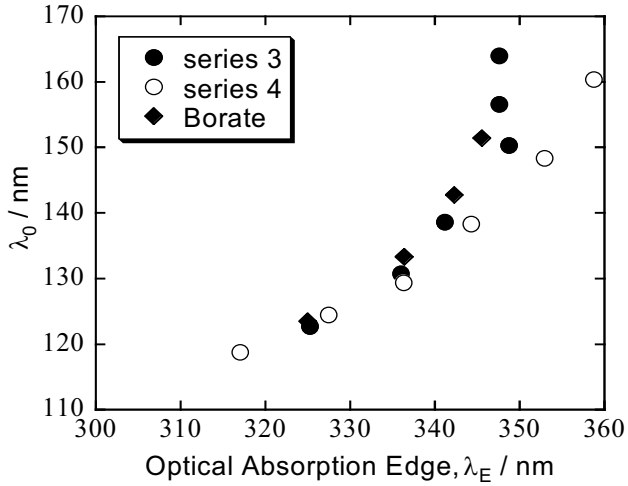

Figure 4: Correlation between the average resonance wavelength λ_0 and the optical absorption edge, λ_E.

Figure 5 shows the correlation between the refractive index n at λ = 632.8 nm and the Abbe number, ν_d. In the glasses with higher refractive index (higher TiO_2 content), Abbe number is small, which means that the wavelength dispersion of refractive index is large. In the titanosilicate glasses of series 3 and 4, a common correlation is clearly seen, and in the titanoborate glasses, however, the correlation is different from the titanosilicate glasses. It is also found from Fig. 5 that the titanoborate glasses show higher dispersion than the titanosilicate glasses.

As indicated in Eq. 5, Abbe number is associated with $1/\lambda_0^2$, and hence the correlation between Abbe number and $1/\lambda_0^2$ is examined. As shown in Figure 6, a linear correlation is observed in all the glasses, suggesting that Abbe number of glass is strongly dependent on the resonance wavelength λ_0, that is, glasses with longer λ_0 have smaller ν_d and higher dispersion.

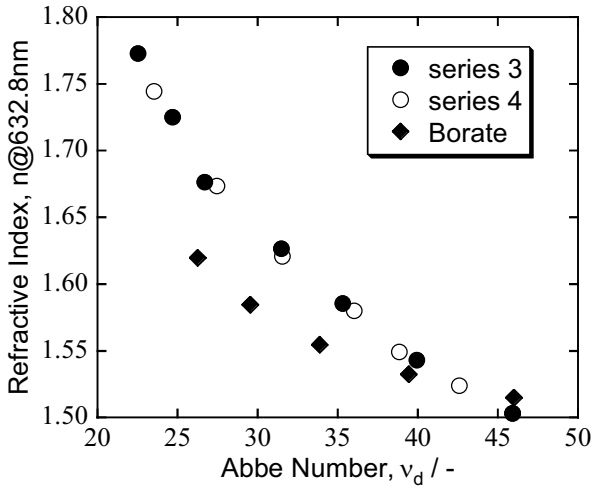

Figure 5: Correlation between refractive index, n and Abbe number, ν_d.

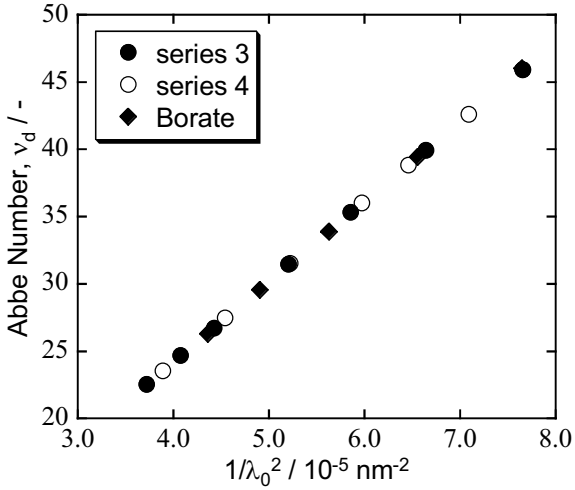

Figure 6: Correlation between Abbe number and $1/\lambda_0^2$.

4.3 Glass Structure

In the present glasses, various oxygen sites are expected, that is, BO sites such as Si–O–Si, Si–O–Ti and Ti–O–Ti and NBO sites as Si–O–Na and Ti–O–Na. When Ti ions act as network modifier, some Si–O–Ti and Ti–O–Ti bonds should be regarded as NBOs. Then, O1s spectra were measured with XPS to classify the oxygen sites in the glasses. Figure 7 shows the O1s XPS spectra for the glasses in series 4.

In the glass at $x = 0$, which is TiO_2-free $Na_2O{\cdot}2SiO_2$ glass, the O1s signal consists of two components, where the higher and lower binding energy components are attributed to BO in Si–O–Si bridging bonds and NBO in Si–O–Na terminal bonds, respectively. The compositional change in the low binding energy component in O1s XPS signal is shown in Figure 8. In series 3, with increasing x, that is, along with the substitution of TiO_2 for SiO_2, the relative intensity of the low binding energy component increases continuously. In series 4, however, with increasing x, that is, along with the TiO_2 addition, the low energy component initially decreases and then shifts to increase in its relative intensity.

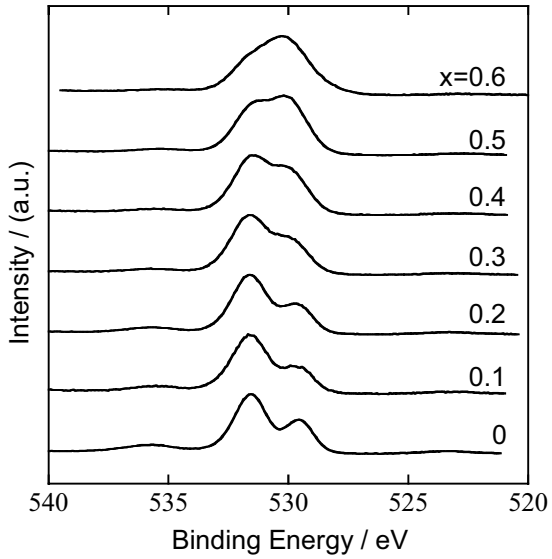

Figure 7: O1s XPS spectra for the glasses in series 4: $x_4TiO_2{\cdot}(1{-}x_4)\{Na_2O{\cdot}2SiO_2\}$.

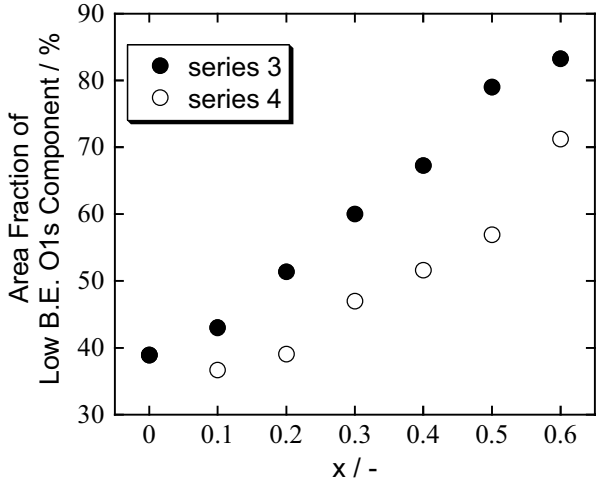

Figure 8: Area fraction of the lower binding energy component of O1s signal in the glasses of series 3: $Na_2O{\cdot}2\{x_3TiO_2{\cdot}(1{-}x_3)SiO_2\}$ and series 4: $x_4TiO_2{\cdot}(1{-}x_4)\{Na_2O{\cdot}2SiO_2\}$

Coordination structure of Ti has been investigated with Raman scattering spectroscopy in Na_2O-TiO_2-SiO_2 glasses [3,7]. Then, Raman spectra of the present glasses were measured, and the intensity was corrected according to the Bose-Einstein thermal population [8]. Figure 9 shows the reduced Raman spectra for the glasses in series 3. The Raman bands were assigned by referring to the

Raman spectra of some crystals, such as Na_2TiSiO_5, TiO_2 (rutile), Ba_2TiO_4, $K_2Ti_2O_5$. The peaks at 880, 750 and 700 cm^{-1} are assigned to TiO_4, TiO_5 and TiO_6 units, respectively. With substituting TiO_2 for SiO_2, the Raman band at around 1100 cm^{-1} due to Si–O bonds decreases and those due to Ti–O bonds increase in intensity. In the low TiO_2 glasses, only the Raman band of TiO_4 unit is observed, and the Raman bands of TiO_5 and TiO_6 units are also confirmed in the high TiO_2 glasses.

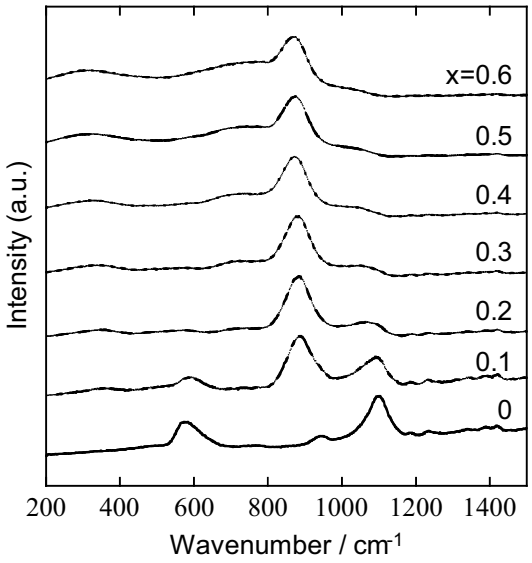

Figure 9: Raman spectra for the glasses in series 3: $Na_2O{\cdot}2\{x_3TiO_2{\cdot}(1-x_3)SiO_2\}$.

As shown in Figure 10, the Raman spectra were separated into Gaussian peaks to obtain the area fraction of the Raman bands of Ti–O bonds. As shown in Figure 11, the Raman band of TiO_4 unit decreases in relative intensity and those of TiO_5 and TiO_6 units increases with increasing TiO_2 content.

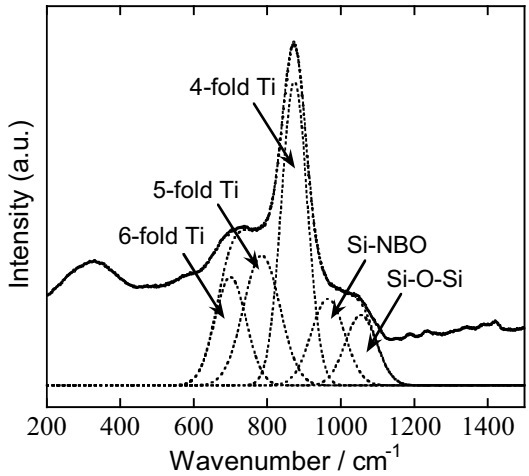

Figure 10: Raman spectrum for $0.4TiO_2{\cdot}0.6(Na_2O{\cdot}2SiO_2)$ glass and its peak separation.

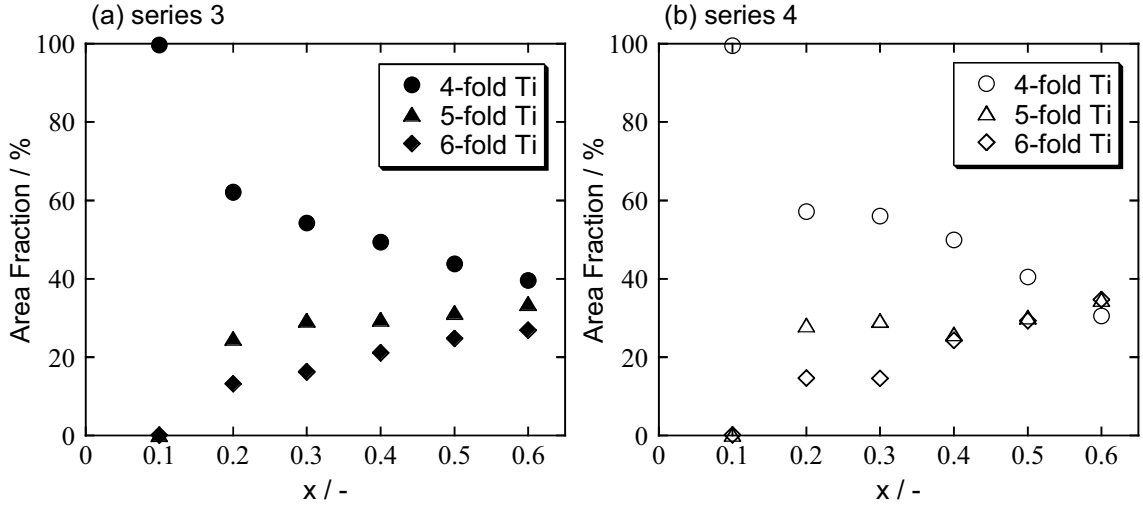

Figure 11: Area fraction of the Raman bands for the glasses of series 3: $Na_2O{\cdot}2\{x_3TiO_2{\cdot}(1{-}x_3)SiO_2\}$ and series 4: $x_4TiO_2{\cdot}(1{-}x_4)\{Na_2O{\cdot}2SiO_2\}$.

Structure of SiO_4 units was evaluated from ^{29}Si MAS NMR analyses. Figure 12 shows the area fraction of the Q^n units in the NMR spectra, where Q^n represents the SiO_4 units containing n BOs and $(4{-}n)$ NBOs. As expected, in the TiO_2-free glasses ($x = 0$), Q^3 units are most abundant, and the compositional change in the relative abundance is different between series 3 and 4. In series 3, Q^3 units decrease and Q^2 units increase in the relative abundance with substituting TiO_2 for SiO_2, indicating the dissociation of bridging bonds and formation of NBOs. In series 4, however, the area fraction of the Q^n units is almost constant despite the compositional change, suggesting that the local structure around Si remains unchanged during the TiO_2 addition. Na/Si atomic ratio is constant in series 4 but is not constant in series 3. If the glass were separated into the glass phases of $Na_2O{-}SiO_2$ and TiO_2, the NMR results would be explainable.

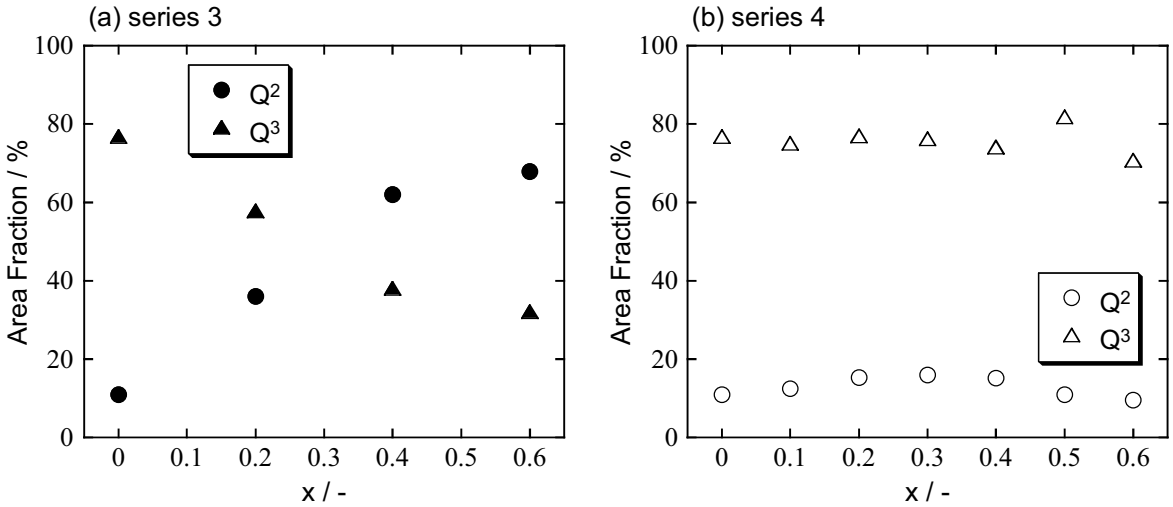

Figure 12: Area fraction of Q^2 and Q^3 SiO_4 components in the ^{29}Si MAS NMR spectra for the glasses of series 3: $Na_2O{\cdot}2\{x_3TiO_2{\cdot}(1{-}x_3)SiO_2\}$ and series 4: $x_4TiO_2{\cdot}(1{-}x_4)\{Na_2O{\cdot}2SiO_2\}$.

In series 4, phase separation was apparently suggested from NMR analysis. However, the structural changes around oxygen and Ti atoms were obviously recognized in the XPS and Raman spectra of the glasses in series 4. Then, the area fraction of the low binding energy O1s component was estimated

based on the following assumptions.

1) 4-fold Ti atoms play as NWF. BOs and NBOs in TiO_4 units indicate the same binding energies of the respective oxygen atoms in SiO_4 units.
2) In TiO_5 unit, oxygen atom in the axial Ti–O bond is a constituent of the low binding energy component in the O1s XPS signal. Oxygen atoms in the equatorial Ti–O bonds are regarded as BOs, and hence they would be included in the high binding energy component. However, the equatorial Ti–O bonds in Na_2TiSiO_5 are ~0.20 nm, which are almost the same with the Ti–O bonds in TiO_6 units in $Na_2TiOSi_4O_{10}$. Therefore, if oxygen atoms in TiO_6 units will be included in the low binding energy component, oxygen atoms in the equatorial Ti–O bonds in TiO_5 units should be also included in the low binding energy component. In this time, two Na ions are required to compensate the negative charge of a TiO_5 unit as $[TiO_{4/2}O]^{2-}\ldots 2Na^{+}$.
3) Ti atoms in TiO_6 units play as NWM. Ti^{4+} ion in a TiO_6 unit compensates totally four NBOs possessing a negative unit charge.

If Ti ions in glass are assumed to be in the same coordination number, the area fraction of the low binding energy O1s component f is expressed as follows.

$$f^{(4)} = \frac{2X_{\mathrm{Na}}}{X_{\mathrm{Na}} + 2X_{\mathrm{Ti}} + 2X_{\mathrm{Si}}} \quad f^{(5)} = \frac{2X_{\mathrm{Na}} + 3X_{\mathrm{Ti}}}{X_{\mathrm{Na}} + 2X_{\mathrm{Ti}} + 2X_{\mathrm{Si}}} \quad f^{(6)} = \frac{2X_{\mathrm{Na}} + 4X_{\mathrm{Ti}}}{X_{\mathrm{Na}} + 2X_{\mathrm{Ti}} + 2X_{\mathrm{Si}}} \qquad (6)$$

where $f^{(4)}$, $f^{(5)}$ and $f^{(6)}$ are the area fraction of the low binding energy O1s component for the cases that all Ti ions are only in 4-fold, 5-fold and 6-fold coordination, respectively. X_{Na}, X_{Ti} and X_{Si} indicate the molar ratios of Na_2O, TiO_2 and SiO_2. As shown in Figure 13, the experimental values (solid circles) are far from either model (lines) in the high TiO_2 regions, suggesting the coexistence of Ti ions in different coordination numbers.

Then, assuming that the relative intensity of the Raman bands for TiO_n units was proportional to the relative amount of TiO_n units, area fraction of O1s low energy component was estimated by combining the results shown in Fig. 11 and Eq. 6. As shown in Fig. 13, the estimated area fractions of the low binding energy component (open triangles) are in good agreement with the experimental fractions for both series, indicating that the assumptions are not widely wrong.

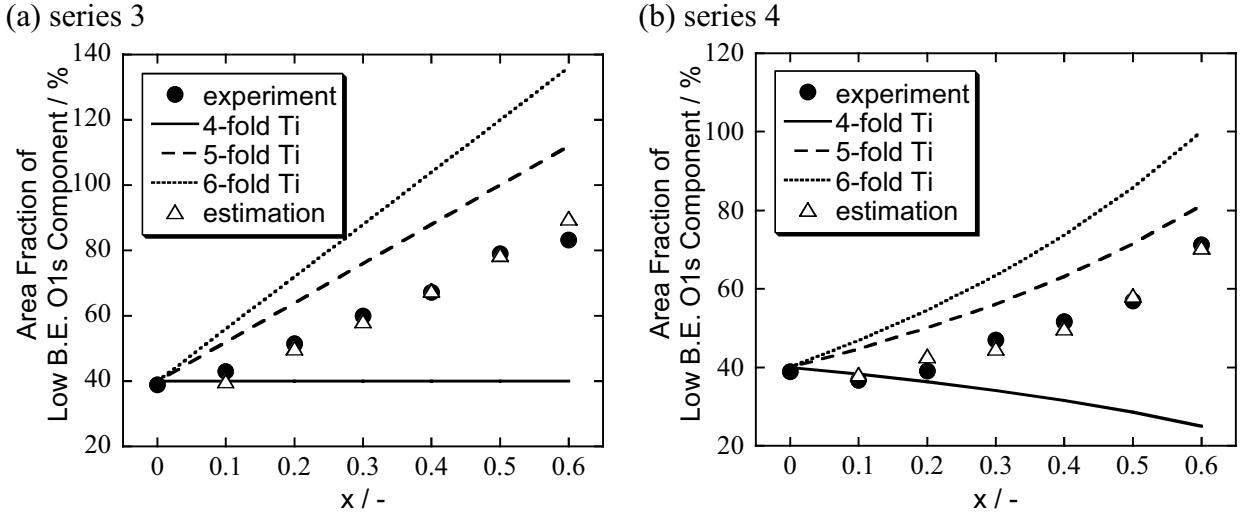

Figure 13: Area fraction of the low binding energy O1s component for the glasses of series 3: $Na_2O{\cdot}2\{x_3TiO_2{\cdot}(1{-}x_3)SiO_2\}$ and series 4: $x_4TiO_2{\cdot}(1{-}x_4)\{Na_2O{\cdot}2SiO_2\}$.

5. Conclusion

In R_2O–TiO_2–SiO_2 glass systems, refractive index and dispersion were investigated based on the single-oscillator Drude-Voigt equation. The refractive index and dispersion were successfully described by the Drude-Voigt equation. Among the parameters in the Drude-Voigt equation, the average resonance wavelength λ_0 was the predominant parameter for both the refractive index and Abbe number. According to Raman spectra, relative amount of TiO_n units was estimated, where with increasing TiO_2 content, the relative amount of TiO_4 units decreased, and those of TiO_5 and TiO_6 units increased. Assuming that oxygen atoms in TiO_5 and TiO_6 units contributed the low binding energy components in O1s XPS signal, the area fraction of the low binding energy O1s component was successfully reproduced. It had been supposed that some relation was present between the average resonance wavelength λ_0 and the glass structure, but no distinct evidence was obtained.

References

1. S. Sakka, F. Miyaji, K. Fukumi, “Structure of binary K_2O-TiO_2 and Cs_2O-TiO_2 glasses,” J. Non-Cryst. Solids, 112 (1989), 64-68.
2. S. Sakka, F. Miyaji, K. Fukumi, “Study on the structure of $K_2O{\cdot}2TiO_2$ glass by X-ray radial distribution analysis,” J. Non-Cryst. Solids, 107 (1989), 171-177.
3. K. Kusabiraki, “Infrared and raman spectra of vitreous silica and sodium silicates containing titanium,” J. Non-Cryst. Solids, 95&96 (1987), 411-418.
4. T. Mito et al., “Effect of high valency cations on high refractive-index and low dispersion characteristics of borate glasses,” J. Ceram. Soc. Japan, 102[12] (1994), 1163-1167.
5. S. Fujino, H. Takebe, K. Morinaga, “Effect of PbO, Bi_2O_3 and Tl_2O on optical properties of heavy metal gallate glasses,” J. Ceram. Soc. Japan, 103[4] (1995), 340-350.
6. S. Hirota, T. Izumitani, R. Onaka, “Reflection spectra of various kinds of oxide glasses and fluoride glasses in the vacuum ultraviolet region,” J. Non-Cryst. Solids, 72 (1985), 39-50.
7. L.A. Farrow, E.M. Vogel, “Raman spectra of phosphate and silicate glasses doped with the cations Ti, Nb and Bi,” J. Non-Cryst. Solids, 143 (1992), 59-64.
8. R. Shuker, R.W. Gammon, "Raman-Scattering Selection-Rule Breaking and the Density of States in Amorphous Materials," Phys. Rev. Lett. 25 (1970), 222-225.